# 5

# Assembling Planetesimals and Planets

We discuss the formation of a dusty accretion disk around an infant star and, from that, the planets. Telescopic observations of young stars suggest planet formation required only a few tens of millions of years, in agreement with a Solar System timescale based on measurements of radioactive isotopes in meteorites. The age of the Solar System, 4.567 billion years, is determined from calcium–aluminum inclusions (CAIs), the first-formed solids. Numerical simulations of planetary accretion further support this timescale and constrain the widths of feeding zones. The compositions of the terrestrial planets are broadly chondritic, but depletions in volatile elements suggest their assembly from already differentiated planetesimals. The ice giants have rocky cores that directly accreted nebular ices, and the even more massive gas giants have ice giant-like cores that swept up nebular gas. Leftover planetary building blocks – asteroids and comets – provide more detailed insights into planet formation processes. We complete this story by discussing the origin of the Moon by a giant impact, and the related topic of orbital perturbations possibly caused by migrations of the giant planets.

## 5.1 Dust to Disk

The origin of the Sun's planetary system has captured scientists' attention for centuries. Our modern understanding comes in part from constraints on processes, compositions, and chronology provided by studies of nebular materials in our own Solar System. Complementing this approach are astronomical observations of other solar systems at various evolutionary stages, as well as numerical models of the assembly of planets from gas and dust. These different approaches provide views of the solar nebula from inside and out. In this chapter, we will consider all these ways of studying planet formation.

Two actual images of swirling dust around young stars are illustrated in Figure 5.1. A new star will consume almost all of the nebular mass, and the small fraction that remains around the star necessarily acquires most of the system's angular momentum. In these images, the orbiting clouds of dust have become flattened into rotating **accretion disks** as dust settles to the nebular midplane. In contrast to these fuzzy images, an artist's conception of the solar nebula (Figure 5.2) suggests a rather turbulent dust disk. Our Sun's retinue of planets somehow emerged from such a debris-laden nebula. Let's see how this happened.

## 5.2 Stages of Accretion

Planets form around young, rapidly evolving stellar objects, and the stages of planet formation can be related to the evolution of their parent stars.

### 5.2.1 Evolution of Stellar Objects

The process of star formation can be inferred from observations of stellar objects at various evolutionary stages.

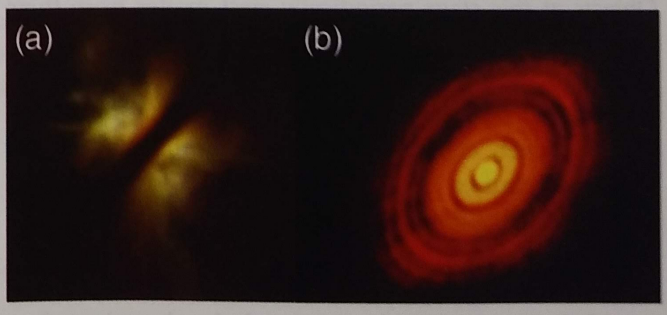


**Figure 5.1** Two images of real accretion disks around young stars. (a) Star HH-30, viewed edge-on, is an image from the Hubble Space Telescope. (b) HL Tauri, from the Atacama Large Millimeter Array, shows gaps that were probably opened by unseen planets.

**Figure 5.2** Artist's rendition of a turbulent solar nebula.

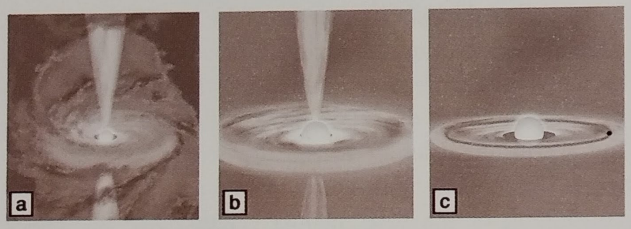


**Figure 5.3** Sketches of the evolution of stellar objects. (a) FU-Orionis stage, in which the protostar is enclosed in an optically thick nebula. (b) Classic T-Tauri stage, in which the gas and dust have formed an accretion disk. (c) Naked T-Tauri stage, in which accretion onto the star has ceased and the formation of planetesimals has cleared the gas and dust. After McSween and Huss (2010).

In the first stage, a young protostar rapidly accretes matter from the enclosing nebula. At this stage, we cannot actually see the star because it is embedded within an optically thick swarm of dust and gas (Figure 5.3a), so the star's energy is irradiated from the nebula itself. Objects at this stage periodically eject matter from their poles; the violent ejections are sometimes called "FU-Orionis outbursts" after the star in which they were first observed. Orbiting particles rotate faster than the gas, so they effectively encounter a "headwind" that slows them down and causes them to drift inward toward hotter regions of the nebula. The formation of water containing isotopically heavy oxygen and the condensation (or evaporation) of solids to form CAIs, both described in Section 4.5, likely occurred in the dusty nebula when the infant Sun was at this stage.

The next stage, called a "classical T-Tauri star" after its type sample, has an optically thick nebula that has been flattened into an accretion disk (Figure 5.3b). Accretion of matter to the star continues, but at a slower rate. This protostar may have bipolar outflows and strong stellar winds. Grains in the disk began to coagulate, and chondrules may have formed at this stage. Clumps of accreted matter grow into **planetesimal** size, and the earliest-formed bodies are heated to the point of melting by the rapid decay of short-lived radionuclides.

A stellar object at the final stage has an optically thin disk (Figure 5.3c), leading to its description as a "naked T-Tauri star." Nebular gas and dust are mostly gone, and the lack of stellar outbursts suggests that the infall of matter into the star has ceased. The formation of larger planetesimals accelerated when the Sun reached this stage, with continued growth forming **planetary embryos** of 100–1000 km in size, which eventually were accreted to form planets. Collectively, this stage and the previous ones took only about ten million years. At this point, the Sun joined the main sequence.

### 5.2.2 Planet Formation

As small planetesimals accrete to form larger objects, gravitational interactions become increasingly important. When the relative velocities of the planetesimals are larger than the escape velocity, accretion occurs with orderly growth. As accretion continues and bodies grow even larger, the relative velocities become less than the escape velocity, favoring runaway growth of the most massive objects as they gobble up the smaller ones (Morbidelli et al., 2012).

The formation of planets from embryos has been studied using numerical simulations, starting with a few dozen objects in initially circular orbits. Close encounters between bodies cause them to be gravitationally perturbed into eccentric orbits that cross each other, allowing the bodies to collide and accrete to form a few planets. The timescale for the formation of planets in stable orbits in these models varies from a few tens of million to 100 million years. The succession of the orderly growth of planetesimals, runaway growth of planetary embryos, and planet formation is called the standard model of planetary accretion.

An example of the output of an accretionary model is illustrated in Figure 5.4a (O'Brien et al., 2006). The system initially contains ~1000 planetesimals with orbits characterized by semi-major axis (distance from the Sun) and eccentricity of their orbits. The simulation shows the progressive coagulation of bodies into a few larger planets with relative diameters indicated by the size of the open circles. Three planets have formed by 10 Ma and continue to grow larger for the rest of the simulation. Such models are stochastic and produce different results each time. Figure 5.4b shows the different planetary systems formed in four simulations; the planets in the model shown in

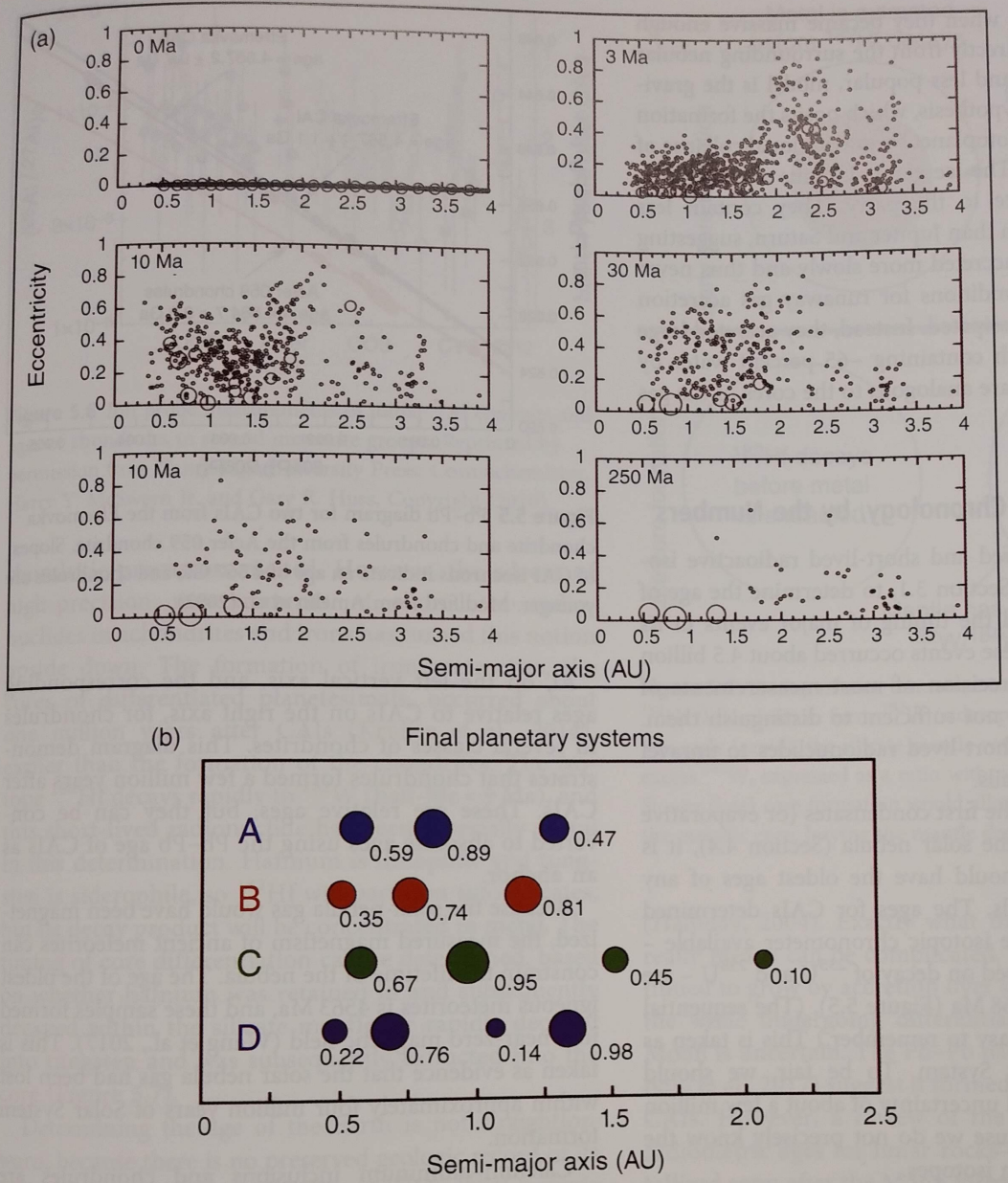


**Figure 5.4** (a) Snapshots of an accretion model for planetesimals that coagulate to form planets (open circles). Orbital semi-major axis (distance from the Sun) and eccentricity for each body are shown in the time progression. (b) Final planetary systems produced by four stochastic simulations; A is the result of the accretion model in (a). The numbers by each planet indicate its mass relative to Earth. Courtesy of D. O'Brien.

Figure 5.4a are system A, and the numbers beside each planet indicate its mass relative to Earth. Such roll-of-the-dice models are sometimes called "Monte Carlo" simulations, after the famous gambling capital. By tracking the fate of each planetesimal, accretion models can also estimate the width of the nebular region from which each growing planet accretes, the so-called "feeding zone."

The accumulation of planetary embryos into planets entailed many collisions between bodies of comparable size. Giant impacts between massive bodies may have stripped off some of Mercury's mantle and formed the Earth's Moon, as described in Section 5.6.

Unlike the terrestrial planets, the gas giants Jupiter and Saturn contain large amounts of hydrogen and helium and must have formed early, while gas was a significant component of the nebula. The favored mechanism for their formation is the core accretion model. The cores initially resembled the rocky terrestrial planets, augmented by

mantles of ices, but when they became massive enough they attracted gas directly from the surrounding nebular disk. A competing, and less popular, model is the gravitational instability hypothesis, which posits the formation of a giant gaseous protoplanet by gravitational collapse of a clump of nebula. The ice giants Uranus and Neptune apparently came late to the party. They contain less hydrogen and helium than Jupiter and Saturn, suggesting that they may have accreted more slowly and thus never quite reached the conditions for runaway gas accretion before the gas was dissipated. Instead, they accreted large amounts of ices, both containing ~65 percent water by mass. The ice giants are analogous to the cores of the gas giants.

## 5.3 Solar System Chronology, by the Numbers

We use both long-lived and short-lived radioactive isotopes, introduced in Section 3.1, to determine the age of the Solar System and the timing of major events in its evolution. Most of these events occurred about 4.5 billion years ago, but the precision of most measurements of long-lived isotopes is not sufficient to distinguish them. To do that, we use short-lived radionuclides to unravel the chronological details.

Because **CAIs** are the first condensates (or evaporative residues) formed in the solar nebula (Section 4.4), it is expected that they should have the oldest ages of any Solar System materials. The ages for CAIs determined from the most precise isotopic chronometer available – the Pb–Pb system, based on decay of $^{235}U$ and $^{238}U$ – are between 4567 and 4568 Ma (Figure 5.5). (The sequential numbers "4567" are easy to remember.) This is taken as the age of the Solar System. To be fair, we should acknowledge an added uncertainty of about a few million years in that age because we do not precisely know the decay rates of uranium isotopes.

Measurements of the decay product of the short-lived radioisotope $^{26}Al$ (half-life = 0.7 Ma) provide further support for the idea of using CAIs to date the Solar System. We know that the $^{26}Al$ was live when the CAIs formed, because its daughter isotope, $^{26}Mg$, is now sited in aluminum-bearing minerals like spinel and hibonite. This nuclide was more abundant in CAIs than in any other Solar System materials, consistent with the early formation of these refractory solids. The former presence of $^{26}Al$ has also been documented in chondrules and in igneous meteorites (achondrites), but always in lower abundances than in CAIs. An example in Figure 5.6 compares the $^{26}Al$ content, expressed as its ratio relative to stable, nonradiogenic

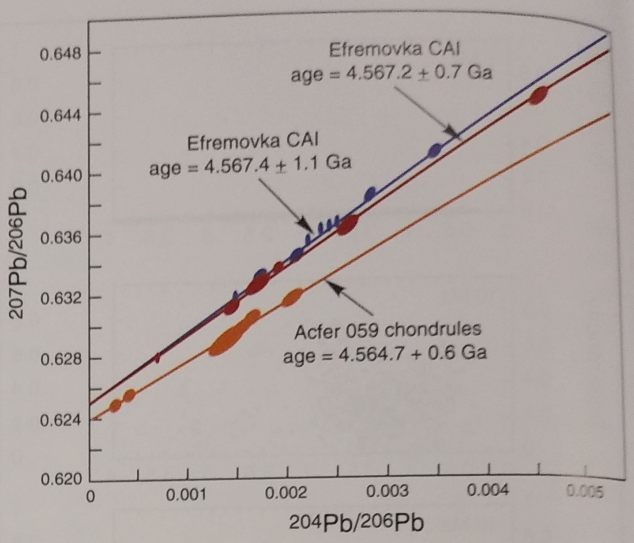


**Figure 5.5** Pb–Pb diagram for two CAIs from the Efremovka chondrite and chondrules from the Acfer 059 chondrite. Slopes of CAI isochrons indicate an age of 4.567 Ga, and chondrules are younger. Modified from Amelin et al. (2002).

$^{27}Al$, on the left vertical axis, and the corresponding ages relative to CAIs on the right axis, for chondrules in several classes of chondrites. This diagram demonstrates that chondrules formed a few million years after CAIs. These are relative ages, but they can be converted to absolute ages using the Pb–Pb age of CAIs as an anchor.

Because the solar nebula gas would have been magnetized, the measured magnetism of ancient meteorites can constrain the lifetime of the nebula. The age of the oldest igneous meteorites is 4563 Ma, and these samples formed in a near-zero magnetic field (Wang et al., 2017). This is taken as evidence that the solar nebula gas had been lost within approximately four million years of Solar System formation.

Calcium–aluminum inclusions and chondrules are components of chondrites. Can we date the time of formation of the chondrites themselves, that is, the accretion ages of chondritic planetesimals? This is tough, because accretion does not reset isotopic chronometers. Accretion must have begun after the chondrules formed, and must have ended by the time of metamorphism or aqueous alteration in parent bodies. Using $^{26}Al$ and other short-lived radioisotopes, the times of chondrite parent body accretion have been bracketed at approximately 4–7 million years after CAIs.

Until recently, planetary scientists believed that the chondrites, composed of nebular materials, accreted early. Melted and differentiated meteorites (achondrites and irons) were thought to have formed later, when

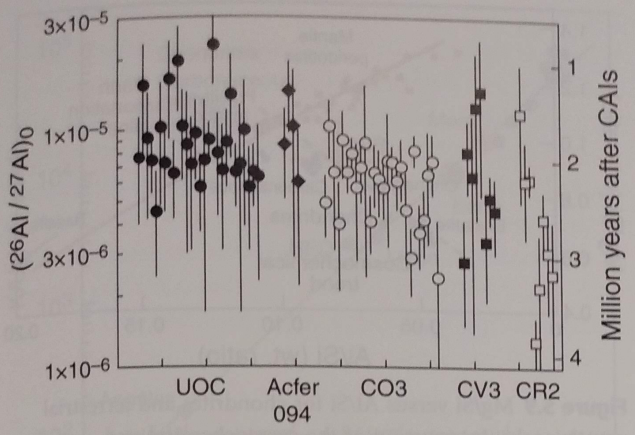


**Figure 5.6** Ion probe measurements of initial $^{26}Al$ contents and ages of chondrules in several meteorite groups. Reprinted by permission from Cambridge University Press: Cosmochemistry, Harry Y. McSween Jr. and Gary R. Huss, Copyright (2010).

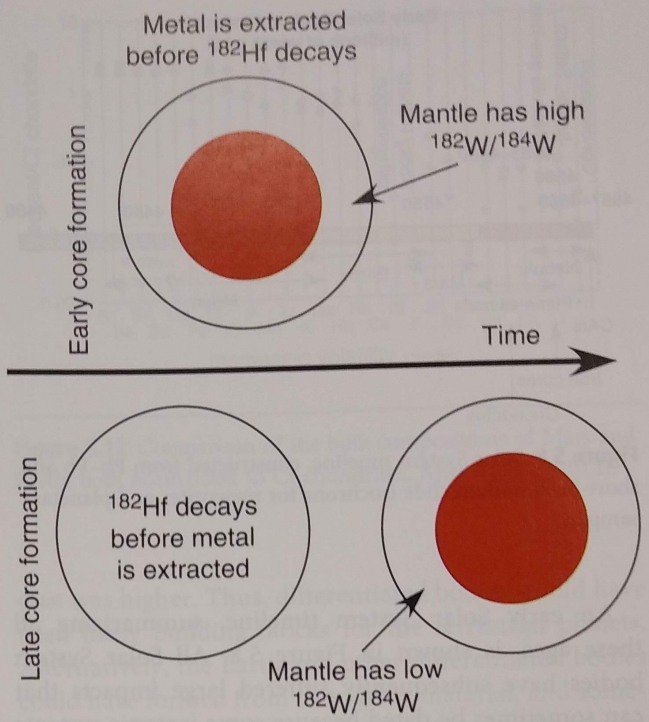


**Figure 5.7** Timing of core formation is revealed by the decay of $^{182}Hf$ (lithophile) to form $^{182}W$ (siderophile). If core formation was early (rapid), the silicate mantle would now contain excess $^{182}W$, expressed as a ratio with nonradiogenic $^{184}W$. Slower (late) core formation would allow $^{182}W$ to partition into the metallic core, leaving the mantle depleted.

chondritic precursors melted. However, the advent of high-precision measurements of short-lived radionuclides in achondrites and irons has turned this notion upside down. The formation of iron meteorites, the cores of differentiated planetesimals, occurred about one million years after CAIs (Kruijer et al., 2014), earlier than the formation of the chondrites. The isotope $^{182}Hf$ decays rapidly to $^{182}W$ (half-life = 9 Ma), and this short-lived radionuclide has been especially useful in this determination. Hafnium is lithophile and tungsten is siderophile, so $^{182}Hf$ will partition into silicates, but its decay product will be concentrated in metal. The timing of core differentiation can be determined, based on whether hafnium was retained in and subsequently decayed within the silicate mantle, or rapidly decayed into tungsten and was subsequently extracted into the core (Figure 5.7).

Determining the age of the Earth is not straightforward, because there is no preserved geologic record of its earliest history. Only the Pb–Pb and $^{182}Hf$–$^{182}W$ isotopic systems provide useful constraints, and both of these systems basically define the time of planetary differentiation. That may not pose a problem though, because of the consensus view that accretion and core formation on the Earth were concurrent. The Pb–Pb age of the Earth, first measured by Claire Patterson in 1956 (recalculated to 4.48 Ga using a new uranium decay constant) postdates the beginning of the Solar System by nearly 100 million years. Subsequently measured Pb–Pb ages are a few hundred million years older than Patterson's date (Tera, 1980). Ages of the Earth determined using the hafnium–tungsten isotopic system are also slightly older, ranging from 11–15 million years after CAIs (Halliday, 2004). Exactly what the "age" of the Earth really means can be complicated, because it likely continued to grow by accretion over some time interval, all the while undergoing differentiation. The age of the Moon is uncertain. The Pb–Pb data for the Moon (Barboni et al., 2017) suggest it formed 60 million years after CAIs. However, a review of the reliability of various radiometric ages for lunar rocks thought to have crystallized soon after the Moon formed indicates a preponderance of younger ages from 4.34 to 4.37 Ga (Borg et al., 2015), which has been used to argue that the Moon formed at least 200 million years after CAIs. An age for Mars determined from $^{182}Hf$–$^{182}W$ in martian meteorites is approximately ten million years after CAIs (Kruijer et al., 2017). The ages of the other terrestrial planets have not been determined, because we have no samples for analysis.

Because Jupiter and Saturn are made mostly of hydrogen and helium, they had to have formed when nebular gas was present. Thus these giant planets accreted rapidly during the first few million years. Uranus and Neptune must have formed more slowly or later.

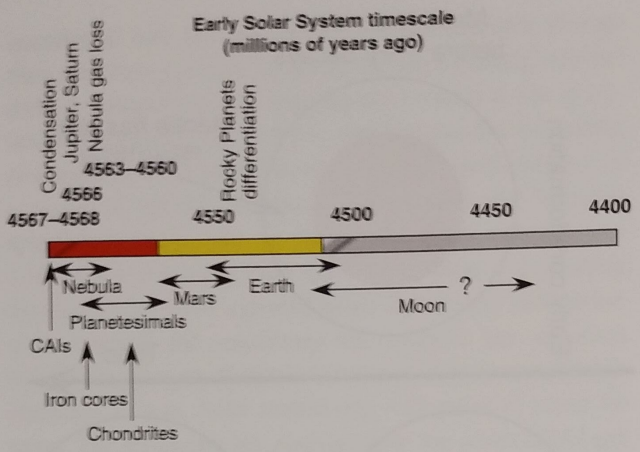


**Figure 5.8** Solar System timeline, constructed from Pb–Pb and short-lived radionuclide isochrons for meteorites and planetary samples.

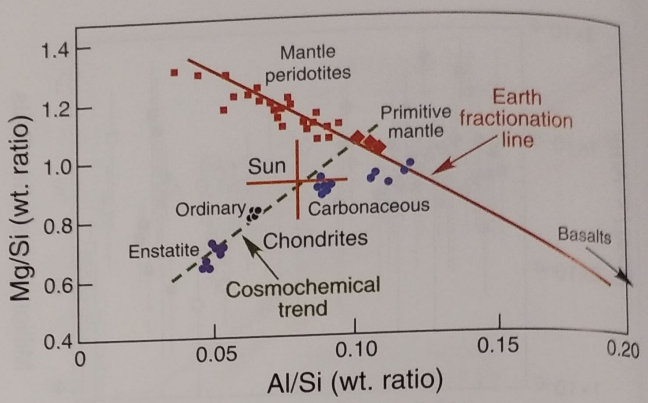


**Figure 5.9** Mg/Si versus Al/Si for chondrites and terrestrial mantle rocks. Intersection of the cosmochemical and fractionation trends serves as an estimate of the primitive mantle composition. Modified from Righter et al. (2006).

An early Solar System timeline, summarizing all these ages, is shown in Figure 5.8. All Solar System bodies have subsequently suffered large impacts that can sometimes be dated because some isotopic systems are reset by shock. Earlier in Section 5.2, we attempted to identify specific processes like condensation and planetesimal accretion with the astronomical stages of the Sun. That connection, rough at best, utilized the relative ages portrayed in this timeline and took into account the thermal and dynamic characteristics of the Sun's stages.

## 5.4 Recipes for Planets

In order to understand the materials that accreted to form a planet, we must determine its bulk composition. However, a differentiated planet's bulk composition must be estimated indirectly because there are no samples anywhere on or within it that represent the entire body.

### 5.4.1 The Terrestrial Planets

Let's focus initially on the Earth's composition, since it is the composition that is best constrained. The Earth is commonly assumed to be broadly chondritic in composition, based on the ratios of refractory elements that have similar geochemical characteristics and thus should not be fractionated from each other during planetary processes.

The Earth is mostly oxygen, magnesium, silicon, and iron, like chondrites. Nearly 80 percent of our planet's iron is in the core, so it must have been accreted as metal, and metal is abundant in some chondrite groups. The Mg/Si and Al/Si ratios of chondritic meteorites and the Sun are illustrated in Figure 5.9. These compositions define a cosmochemical trend. The compositions of peridotites from the Earth's mantle define a terrestrial fractionation trend on this diagram. The intersection of these two trends is taken to represent the Earth's bulk composition. Three published estimates of the primitive (unfractionated) mantle are also shown, and all plot near this intersection. The Earth is most similar to carbonaceous chondrites in terms of these three elements, but its oxygen isotopic composition is like enstatite chondrites and its osmium isotopic composition is like ordinary chondrites. If the Earth is chondritic, it probably formed from some mixture of chondrites like those in our present meteorite collections.

The ratios of refractory and volatile elements having similar geochemical behavior reveals that the Earth is depleted in volatile elements, relative to chondrites. Figure 5.10 illustrates two such ratios of volatile to refractory elements, K–U and Rb–Sr. Each pair of elements travel together during igneous processes, so their ratio remains nearly constant although their absolute amounts may change. From this figure we can see that volatile potassium and rubidium are depleted in the Earth, and in Mars, the Moon, and achondrites (HEDs, angrites) as well, relative to refractory uranium and strontium. This is a general characteristic of all differentiated bodies. Figure 5.11 shows that the depletion of volatiles in the Earth extends to other elements besides potassium and rubidium; volatility in this diagram is indicated by the temperatures at which half of the element condenses from a gas of solar composition. In contrast, refractory elements occur in roughly

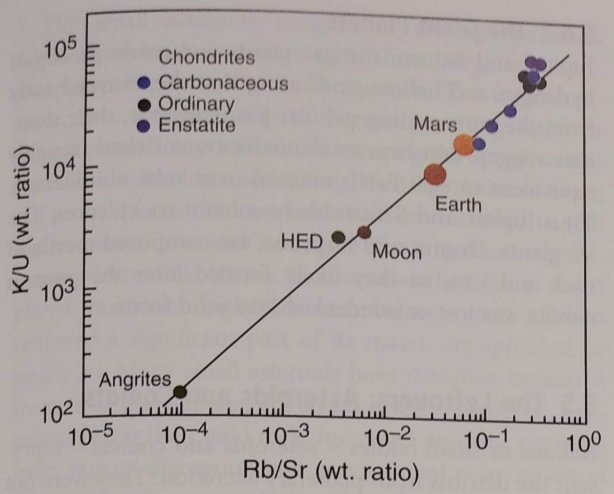


**Figure 5.10** Ratios of volatile (K and Rb) to refractory (U and Sr) elements in meteorites and planets. Planets and differentiated planetesimals (HED and angrite meteorites) are depleted in volatile elements, relative to chondrites. Modified from Tolstikhin and Kramers (2008).

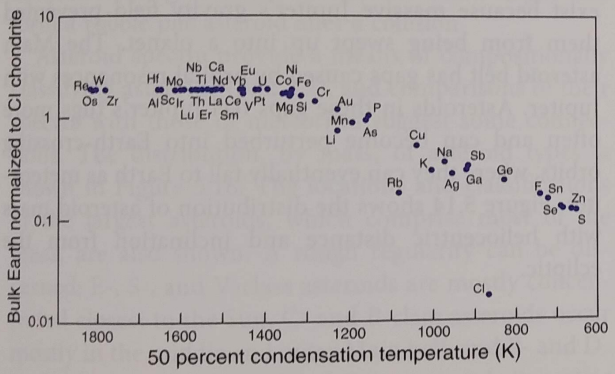


**Figure 5.11** Elemental composition of the bulk Earth, normalized to CI chondrites. The refractory elements, which condense at high temperatures, have nearly chondritic abundances (raised slightly above 1 by the loss of volatiles). Volatile elements are systematically depleted, according to their volatility. After Albarede (2009).

chondritic proportions. The Earth's volatile element depletion could be explained if it accreted in large part from already differentiated planetesimals, rather than from chondrites. In Section 5.3 we learned that the earliest-formed planetesimals melted and differentiated to form cores, and chondritic bodies formed later. These differentiated bodies may have been abundant in the inner Solar System, because accretion is thought to have begun closer to the Sun where the density of

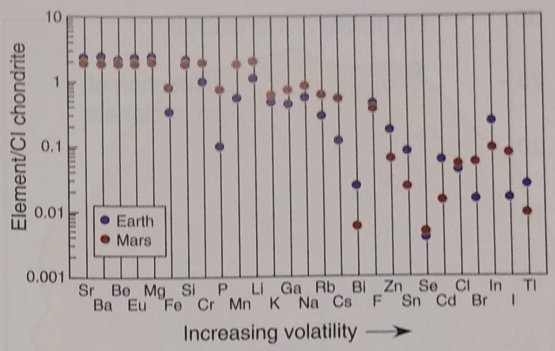


**Figure 5.12** Comparison of the bulk compositions of Mars and Earth, both normalized to CI chondrites. After Taylor (2013).

dust was higher. Thus, differentiated bodies would have been likely building blocks for the terrestrial planets. Alternatively, the Earth and other differentiated bodies could have formed from chondritic material, and somehow lost volatiles during differentiation. In either case, though, the bulk compositions of these bodies would still be chondritic, except for depletions in volatile elements.

Even with unlimited samples to analyze, determining the Earth's bulk composition, as illustrated in Figure 5.11, requires considerable effort. Estimating the composition of other planets is even more challenging. Let's take the case of Mars. Three different approaches have been utilized, with varying success. The first approach mixes chondrite classes (components of the nebula) to produce a planet having element ratios like those in martian meteorites. The second also mixes chondrite classes, but in this case to reproduce the distinctive oxygen isotopic composition of martian meteorites. The third uses geophysical data to estimate how mineralogy varies with depth, and the bulk composition is calculated from the mineralogy. All three approaches give roughly similar results, mainly differing in the degree of volatile element depletion. A recent reassessment of the Mars bulk composition (Taylor, 2013) is compared with that of the Earth in Figure 5.12. The compositions are rather similar, except that Mars has higher concentrations of moderately volatile elements (in the middle of the diagram).

We might expect planetesimals, and the planets made from them, to vary in some regular way with distance from the Sun. If the nebula temperatures decreased outward, planets should show decreasing refractory element abundances and increasing volatile element abundances

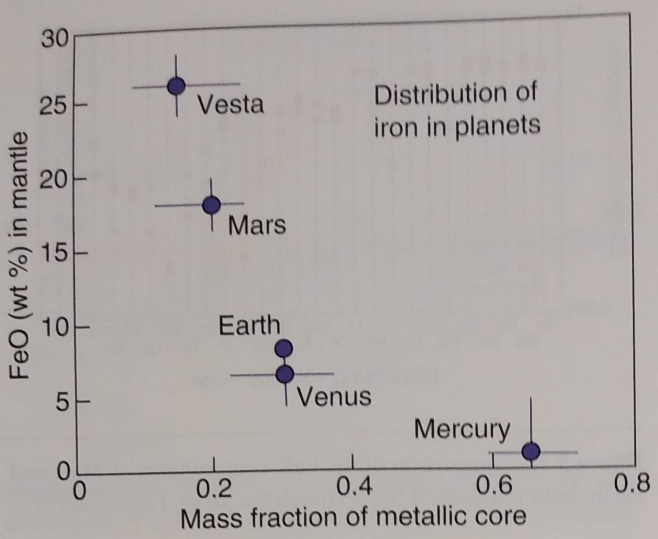


**Figure 5.13** The mass fractions of iron as metal in cores and as FeO in mantles vary systematically in the terrestrial planets and asteroid Vesta. After Righter et al. (2006).

as we move outward from Mercury, to Venus, Earth, and Mars. However, this pattern is not observed. We do observe, however, systematic changes in the oxidation state of these planets. We can see this most readily by comparing the amounts of iron occurring as metal in cores and as FeO in mantles. (We will explain how core masses in other planets are determined in the following chapter.) Mercury has a massive iron core with very little FeO in its mantle, Earth and Venus have intermediate-sized cores, and Mars has a small core and an FeO-rich mantle (Figure 5.13).

### 5.4.2 The Giant Planets

Jupiter and Saturn, the gas giants, are made mostly of hydrogen and helium, indicating that they formed early from the surrounding nebular gas. However, their densities suggest that heavier elements are enriched (roughly equivalent to ~20 Earth masses) over solar abundances. Thus Jupiter and Saturn likely contain rocky cores. The ice giants, Uranus and Neptune, are composed mostly of rock and ices, so they likely formed after the gaseous nebula was lost or condensed into solid form.

## 5.5 The Leftovers: Asteroids and Comets

Billions of small bodies – asteroids and comets – represent the detritus from planetary accretion. They were not used as planetary building blocks, but carry important information about planet formation.

### 5.5.1 Asteroids

Many thousands of unused planetary building blocks litter the asteroid belt and regions around and outside the orbit of Jupiter (Burbine, 2017). These objects still exist because massive Jupiter's gravity field prevented them from being swept up into a planet. The Main asteroid belt has gaps caused by orbital resonances with Jupiter. Asteroids in these gaps feel Jupiter's tugs more often and can become perturbed into Earth-crossing orbits, where they can eventually fall to Earth as meteorites. Figure 5.14 shows the distribution of asteroid mass with heliocentric distance and inclination from the ecliptic.

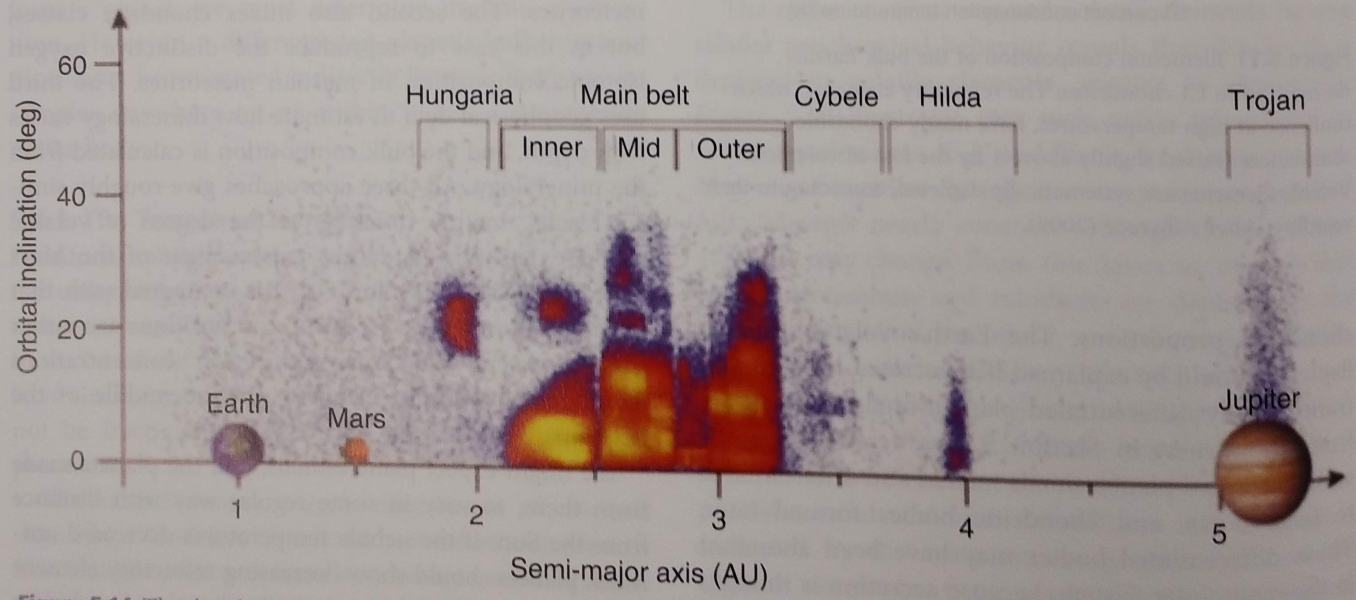


**Figure 5.14** The distribution of mass within the asteroid belt, showing the major divisions and gaps produced by orbital resonances with Jupiter. Modified from DeMeo and Carry (2014).

The small asteroids imaged by visiting spacecraft (shown previously in Figure 1.10) show irregular shapes, as appropriate for collisional fragments. The fragmentations, too, are the result of Jupiter pumping up their orbital eccentricities and thus increasing the opportunities for collision. Phobos and Deimos, the tiny moons of Mars, are probably captured asteroids and are included in that figure. Intact Ceres and Vesta (see Box 5.1), the two most-massive asteroids (Ceres is now classified as a dwarf planet, and Vesta might have been before a giant collision removed a significant part of its mass), are spherical or nearly so. Many small asteroids have densities, estimated from their gravitational effects on nearby spacecraft, considerably less than solid rock. Increased porosity, resulting from impact disruption and gravitational re-accretion of the resulting fragments, is thought to be the likely explanation, although asteroids containing ice as well as rock will also have lower densities. Figure 5.15 illustrates a metamorphosed chondritic asteroid, with internal shells containing different petrologic types, and a rubble pile asteroid consisting of jumbled fragments gravitationally reassembled after collisional disruption. A differentiated body, consisting of core, mantle, and crust, might also form a rubble pile asteroid after a collision.

Asteroid spectra provide a means of compositionally classifying asteroids (Box 2.2), and comparisons of their spectra with those of meteorites suggest some connections. The distribution, by mass, of asteroid types is shown in Figure 5.16. The locations and classifications of the largest asteroids, which comprise most of the mass, are also shown. A rough regularity can be discerned: E-, S-, and V-class asteroids are mostly concentrated closest to the Sun, C- and B-class asteroids occur mostly in the middle and outer Main belt, and P- and D-class asteroids are most abundant at greater heliocentric distance. This distribution may reflect, in part, increased heating nearer the Sun. The innermost bodies were thermally metamorphosed or melted. The E-class asteroids are spectrally similar to enstatite chondrites and their melted equivalents, the aubrites; many S-class asteroids appear to be ordinary chondrites and their partly melted equivalents, the acapulcoites; and V-class asteroids are parent bodies of the igneous eucrites and diogenites. Also occurring in this region but not illustrated in Figure 5.16 are lesser amounts of M-class asteroids, interpreted to be fragments of metallic cores that have been stripped of the overlying silicate mantles. The C- and B-class bodies in the middle belt, spectrally similar to carbonaceous chondrites, once contained ice, which on heating produced aqueous fluids that altered them. Melting the ice used thermal energy, which moderated temperatures in these asteroids. At greater distances ice never melted, so the P- and D-class bodies are relatively unaltered. Meteorites from these bodies have not been recognized, although they may have been sampled as some interplanetary dust particles. The

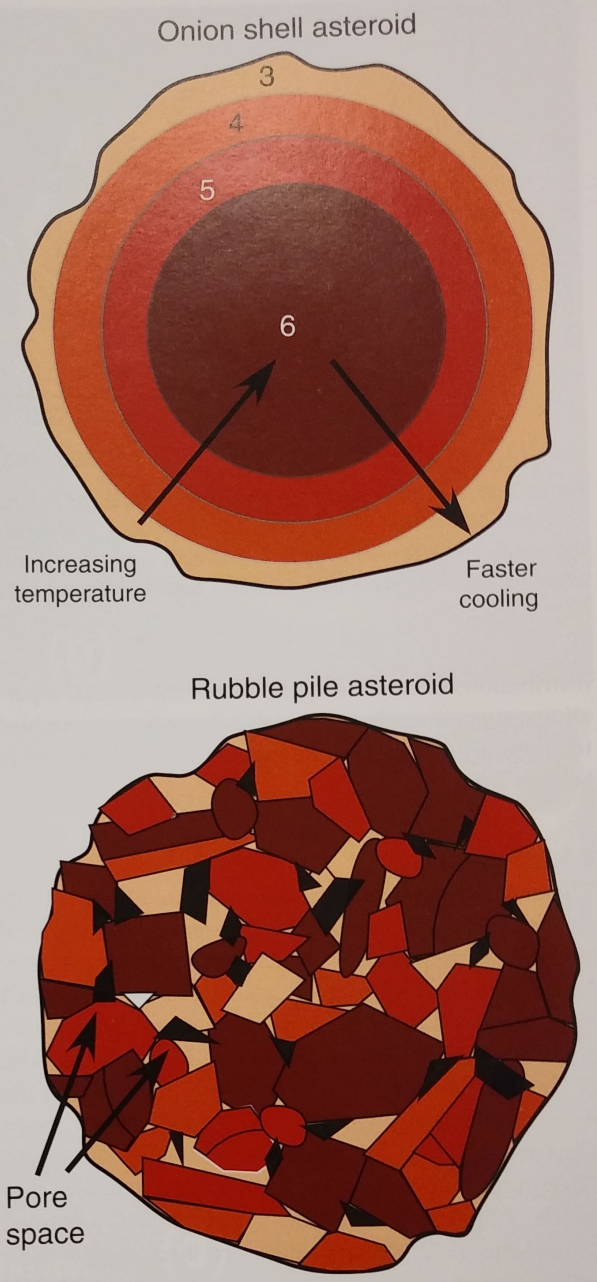


**Figure 5.15** Comparison of structures for chondritic asteroids. The onion shell model has concentric metamorphic zones, with type 6 chondrites in the interior and type 3 on the outside. A rubble pile structure is produced by collisional disruption and reassembly of an onion shell body, jumbling the fragments and adding porosity to the asteroid.

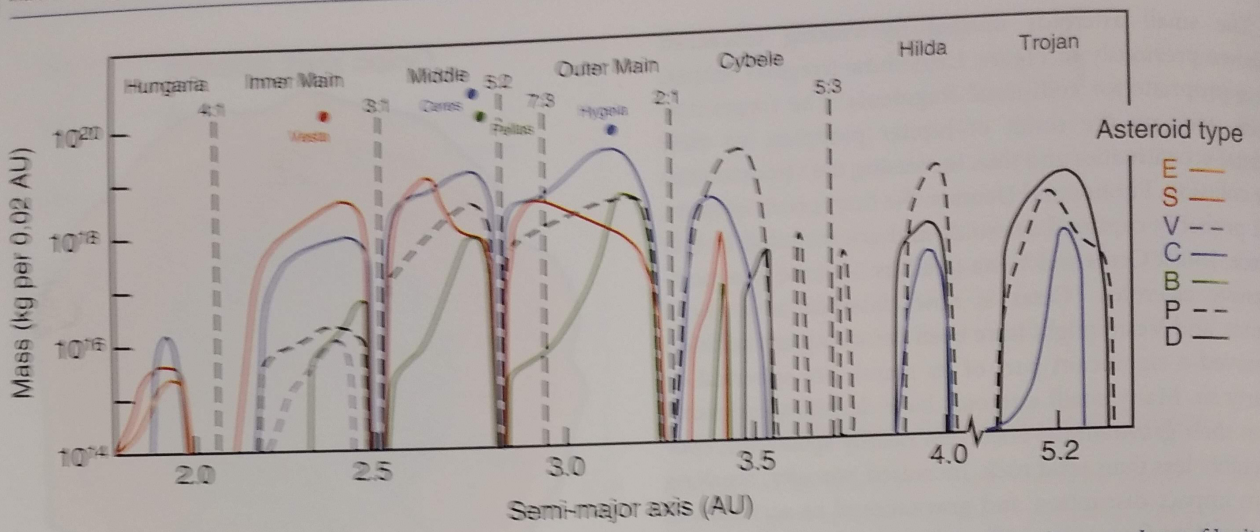


**Figure 5.16** Asteroid spectral classes versus heliocentric distance. Abundances are shown as masses rather than numbers of bodies. A general distribution pattern, with E-, S-, and V-class asteroids occurring closer to the Sun, C- and B-class asteroids concentrated in the middle and outer belt, and P- and D-class asteroids occurring farthest from the Sun, is observed, although the orbits of many asteroids have been scrambled. Modified from DeMeo and Carry (2014).

distributions of asteroid types do not show clean separations, suggesting that their orbits have been scrambled to some degree. A possible explanation is discussed in Section 5.6.

### 5.5.2 Comets

The radial distance at which ice condensed in the nebula is referred to as the **snow line**; determining its actual location is complicated, and its exact position probably varied with time. The giant planets, as well as comet reservoirs, are located beyond the snow line. The sources of comets are the Kuiper belt, located beyond the orbit of Neptune and extending from 30 to 50 AU, and the even more distant Oort cloud. Pluto and its moon Charon are actually the innermost Kuiper belt objects. Current models suggest that most of the icy bodies now in the Kuiper belt and Oort cloud originally formed among the giant planets, but were ejected into these nether regions.

The ices in comets sublimate as they are warmed when perturbed into orbits that bring them closer to the Sun. Their bright appearance, caused by escaping gas and dust, is in stark contrast to the comet nuclei themselves, which are dark as black velvet. Images of comet nuclei visited by spacecraft were shown in Figure 1.11. The dark crusts are apparently lag deposits of dust, and the underlying ice-rich materials only show in outbursts. Comets are weakly consolidated objects with high porosity, and tidal forces during a close encounter with a planet can cause them to split into fragments, as occurred when comet Shoemaker–Levy passed by Jupiter in 1992.

Samples of comet Wild 2 collected and returned to Earth by the *Stardust* spacecraft (Figure 5.17) contain the same minerals found in chondrites (Brownlee, 2014). Surprisingly, some of these minerals occur in CAIs and chondrules, thought to have formed by condensation and melting close to the Sun. The expectation, before this mission, was that comets consisted of ices and tiny interstellar grains with organic mantles. Although this is just one comet, its mineralogy is similar to IDPs that are thought to sample many comets. From this evidence it appears that comets are not as primitive as previously believed, and that nebular materials must have been transported outward over vast distances.

### 5.5.3 A Hole in the Solar Nebula?

Stable isotopic analyses of meteorites and larger bodies for which we have samples (Earth, Moon, Mars, and Vesta) reveal a compositional gap (Warren, 2011; Scott et al., 2018) (Figure 5.20a). The axes of this figure require a little explanation. In Section 4.5, we learned that oxygen has three isotopes, and $\Delta^{17}O$ is the deviation in $\delta^{17}O$ from the terrestrial mass fractionation line. The horizontal axis, $\varepsilon^{54}Cr$, is $^{54}Cr/^{52}Cr$ relative to the ratio in chondrites. Both isotopes are hypothesized to identify materials from different regions of the solar nebula. A number of other isotope ratios, such as $^{50}Ti/^{47}Ti$ and $^{95}Mo/^{94}Mo$, also show a similar

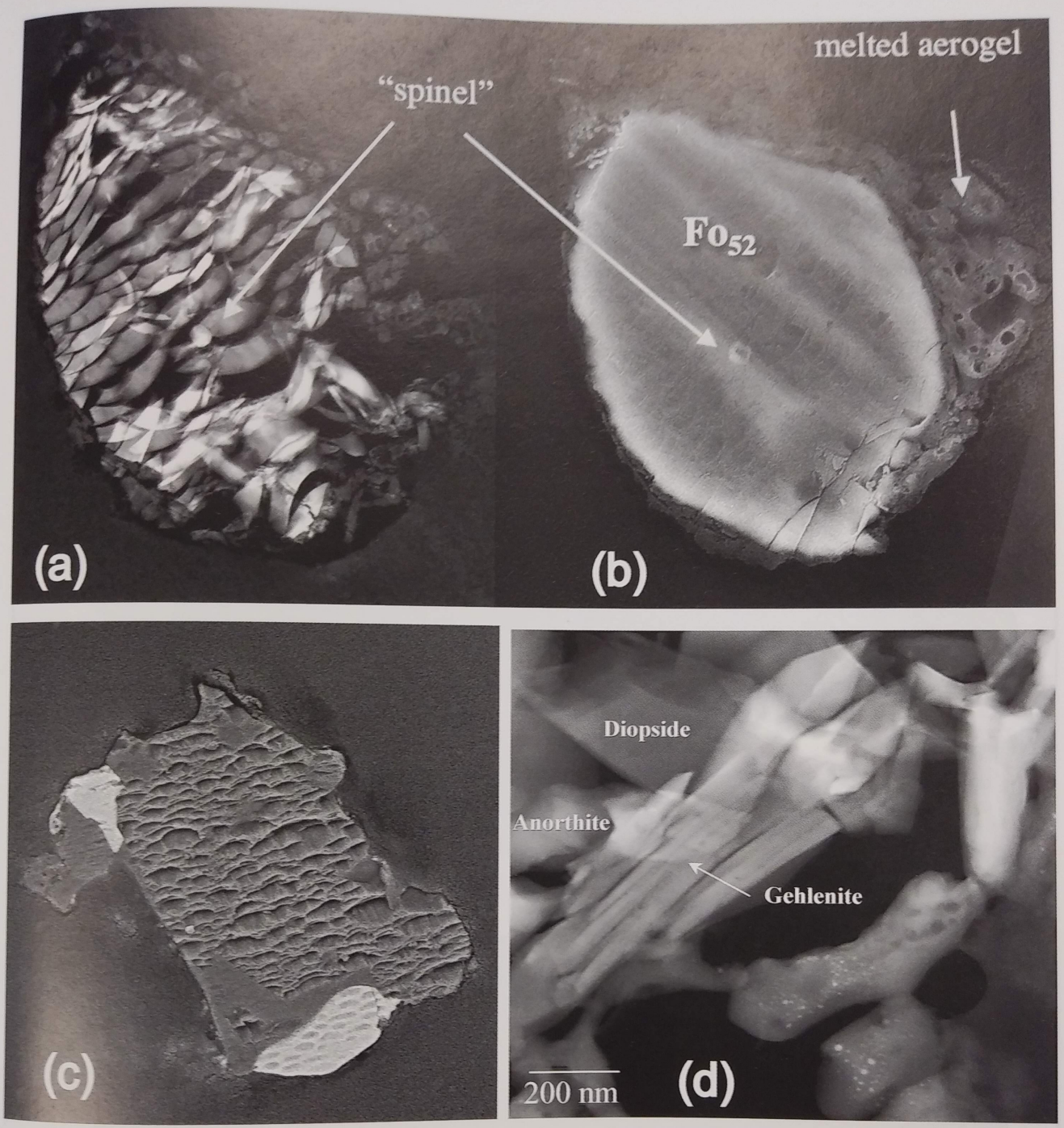


**Figure 5.17** Examples of comet particles collected by the *Stardust* spacecraft. (a,b) Plane-polarized light and SEM (scanning electron microscope) images, respectively of an olivine grain containing spinel, FOV = 4 μm. (c) Particle composed of pyroxene and sulfide, FOV = 1 μm. (d) Particle composed of minerals in CAIs. Images by D. Brownlee; reprinted by permission from Cambridge University Press: Cosmochemistry, Harry Y. McSween Jr. and Gary R. Huss, Copyright (2010).

compositional gap when plotted against $\Delta^{17}O$. This isotopic gap has been interpreted to represent a physical gap in the early nebula, separating regions with distinct compositions.

In this model, the ordinary and enstatite chondrites, the Earth, Moon, Mars, and Vesta, as well as numerous achondrites and irons, formed in the inner Solar System. The carbonaceous chondrites, along with a few types of

## BOX 5.1 FIRE AND ICE: VESTA AND CERES

Vesta (Russell et al., 2015) and Ceres (Russell et al., 2016) are the most massive representatives of only a handful of remaining intact planetesimals. Both asteroids have been explored by the *Dawn* spacecraft, which provided views of the geologic complexity of protoplanetary bodies. Vesta is a differentiated body of rock and metal. In contrast, Ceres has a rocky interior with a large amount, ~25 percent, of ice. These bodies may represent compositional extremes in the asteroid belt, but both kinds of planetesimals must have been building blocks for the Earth.

A **shape model** (Figure 5.18a) illustrates the rugged topography of Vesta's surface. A geologic map of Vesta, compiled using stratigraphic procedures described in Section 3.2, is shown in Figure 5.18b. Cratered highlands in the northern hemisphere represent the oldest crust. The excavation of two giant impact basins, first Veneneia and then Rheasilvia, near the south pole scattered ejecta over the southern hemisphere and produced equatorial girdles of ridges and troughs (the Saurnalia Fossae and Divalia Fossae, respectively). Marcia is among the most recent impact craters on Vesta.

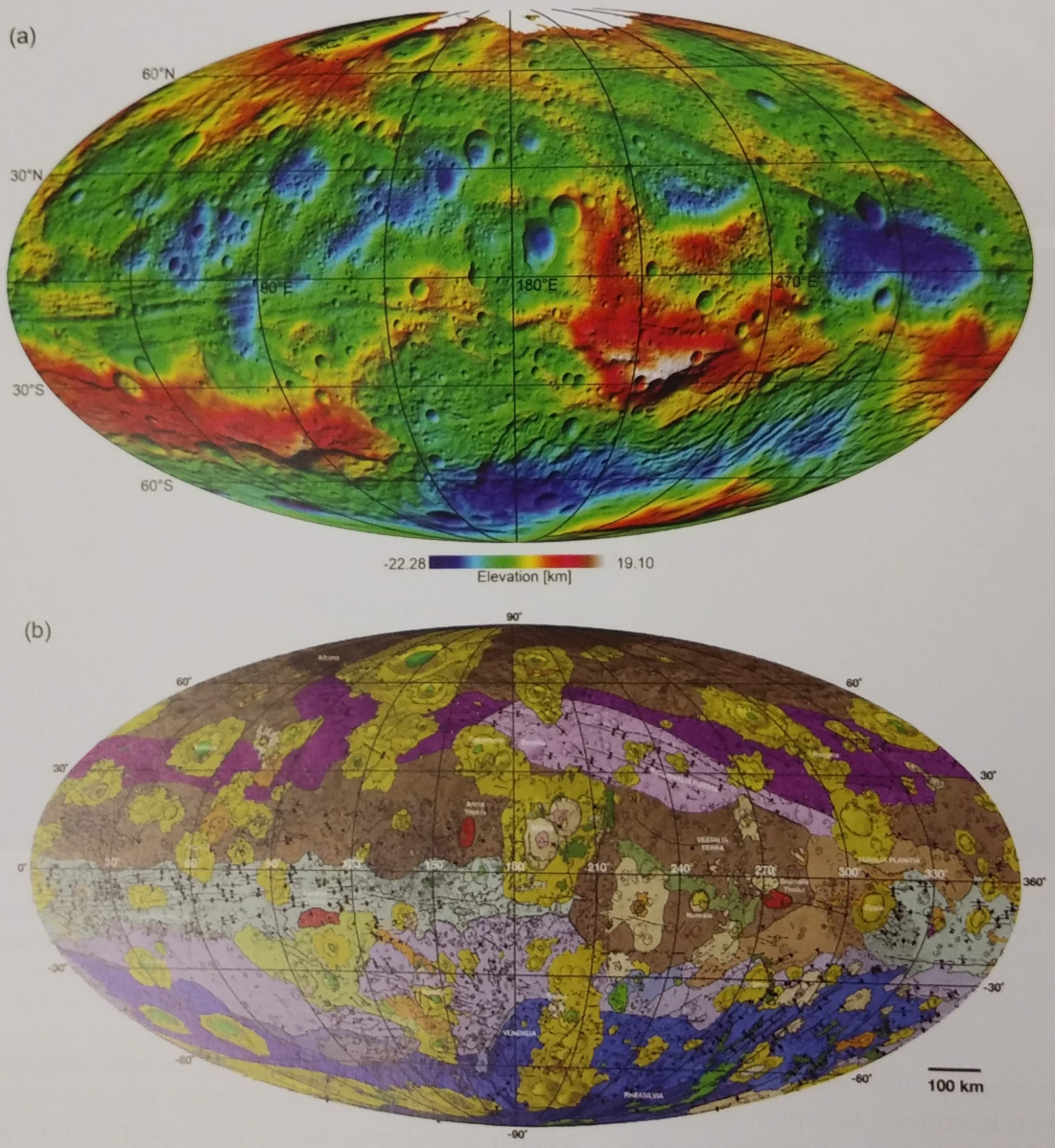


**Figure 5.18** (a) Vesta shape model, showing the rugged topography of the asteroid's surface. (b) Geologic map of Vesta. See Williams et al. (2015) for key to mapped units.

Ceres has an icy mantle with a dark coating of phyllosilicates on the surface. Bright spots are the sites of recent activity that concentrated carbonate minerals. A shape model and geologic map of Ceres are shown in Figure 5.19a,b. It has less topographic relief than Vesta, but the lack of relaxation of its small impact craters requires that its crust contains no more than ~40 percent ice.

Although these rocky and ice-bearing asteroids are distinct, the compositional boundary between asteroids and comets is actually rather fuzzy. A few distant, ice-bearing asteroids show periodic cometary outbursts, and the aqueous alteration experienced by carbonaceous chondrites indicates that many C-class asteroids once contained ice. In the early Solar System, asteroids beyond the snow line may have resembled comets before their ice melted.

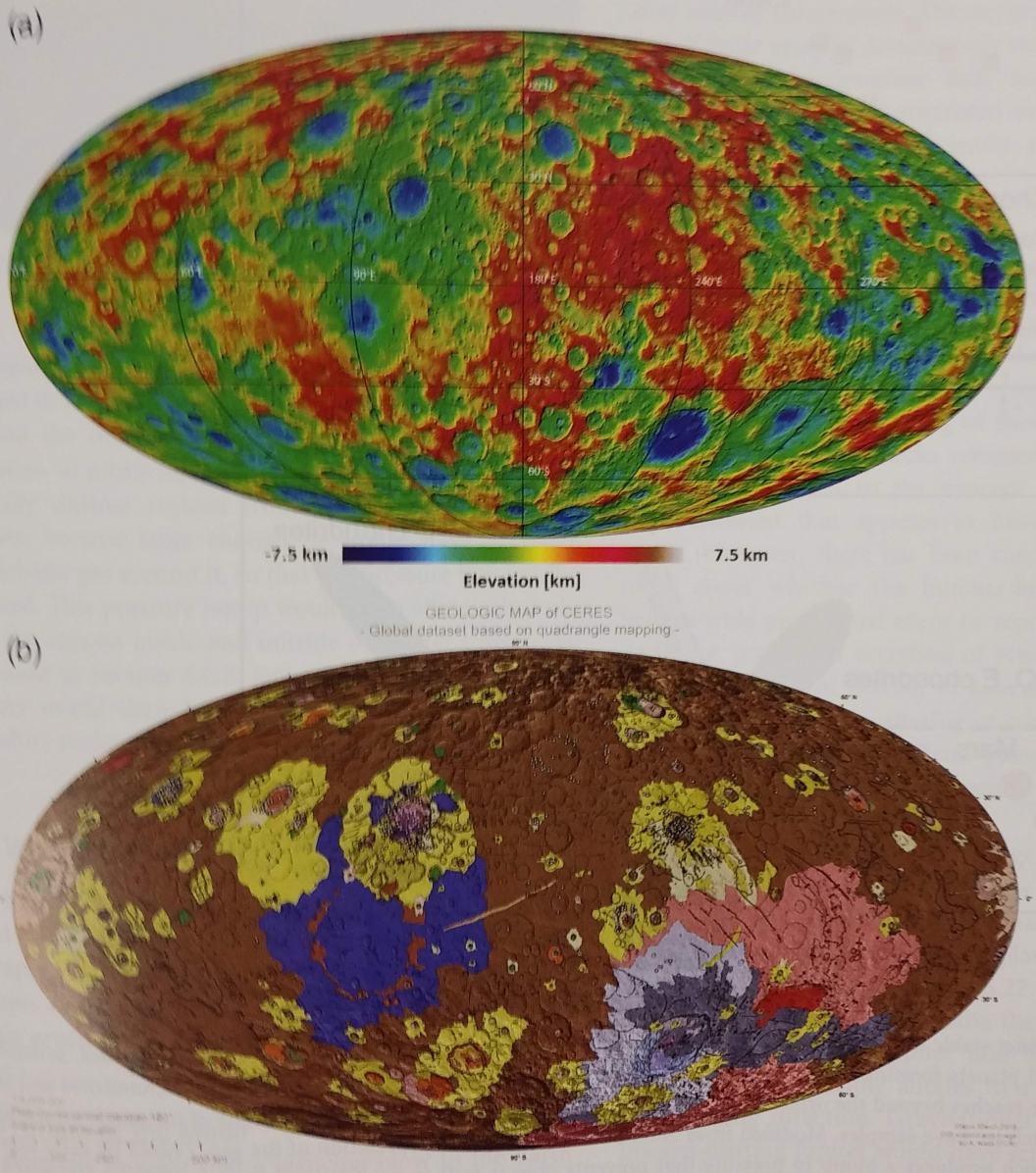


**Figure 5.19** (a) Ceres shape model. (b) Geologic map of Ceres. Adapted from Williams et al. (2018), see that reference for key to mapped units.

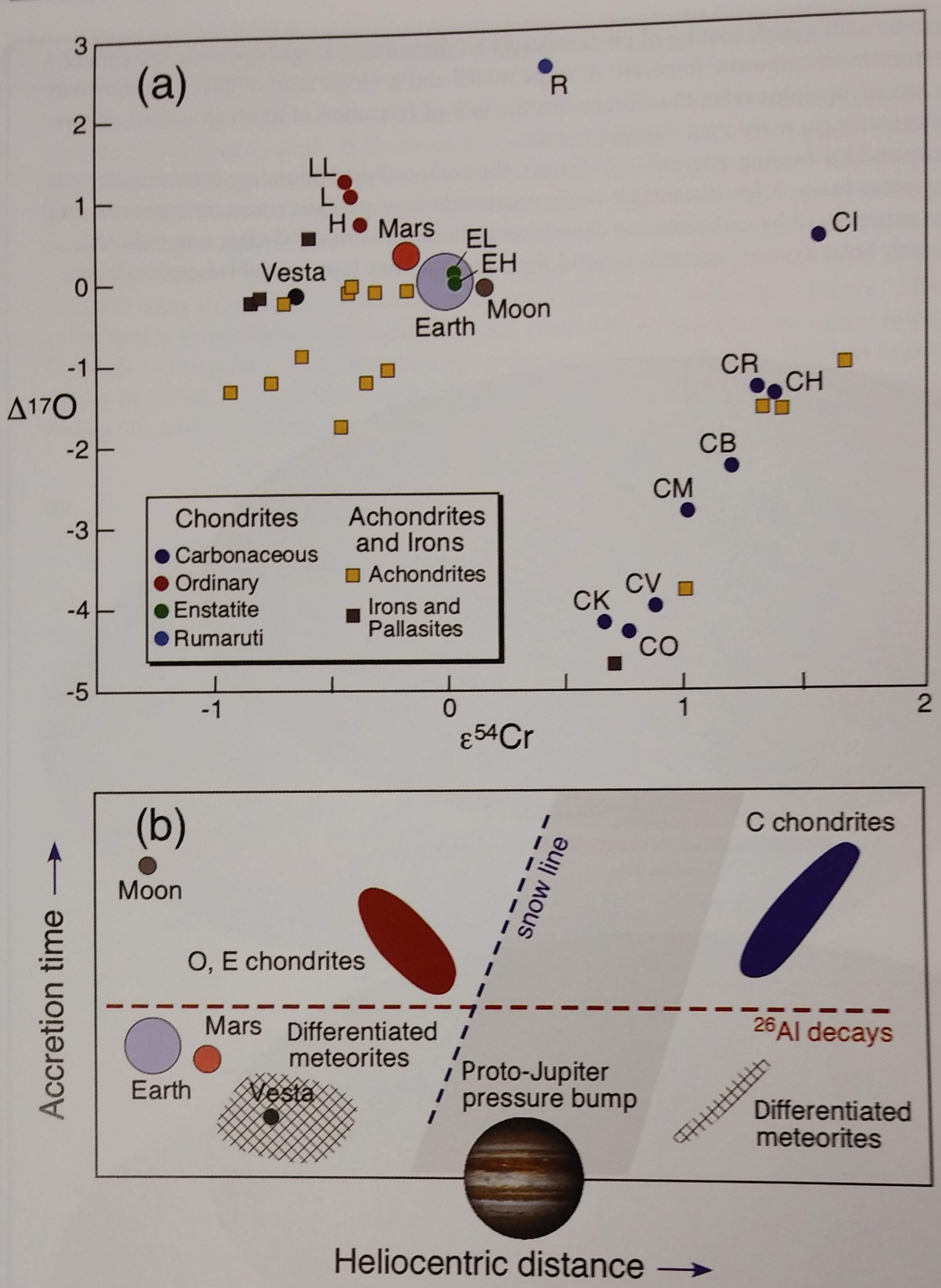


**Figure 5.20** (a) Distinct stable isotopic compositions may point to a gap in the solar nebula, with most chondrites, achondrites, irons, and terrestrial planets forming in the inner Solar System, and carbonaceous chondrites and some achondrites and irons forming in the outer reaches beyond the orbit of Jupiter. The diagram shows the average compositions of meteorite groups and of other bodies for which we have samples. Modified from Scott et al. (2018). (b) Interpretation of the gap, caused by early accretion of proto-Jupiter, which produces a bump in pressure that prevents objects farther out from entering the inner Main belt and terrestrial planet region. Bodies outboard of the snow line contain ices. Bodies that accreted early, before too much $^{26}$Al decayed, experience melting and differentiation, whereas those that accreted later experienced thermal metamorphism or aqueous alteration.

**Figure 5.21** Artist's depiction of the Moon-forming impact.

oxidized achondrites and irons, are interpreted to have formed in the outer Solar System, past the snow line and beyond the orbit of Jupiter (Figure 5.20b). The early accretion of proto-Jupiter may have kept these compositionally distinct regions from mixing. Once Jupiter's nucleus became large enough, it would have accreted the nebular gas around it, so that gas pressure was locally lowered. This pressure bump would have effectively isolated the regions inside and outside of Jupiter's orbit. As discussed in Section 5.6.2, later migrations of the giant planets would then have implanted the carbonaceous chondrite bodies into the asteroid belt.

## 5.6 Whence Earth's Moon?

The Earth's Moon is unique, in that it is so large compared to its neighboring planet. The origin of the Moon has captivated scientists' imagination, and its explanation prompts novel ideas about the scale and importance of impact processes in the early Solar System.

### 5.6.1 Origin of the Moon

It is generally thought that a glancing blow to the Earth by a Mars-sized impactor (Figure 5.21) produced fragments and vaporized material that went into orbit around the Earth and subsequently accreted to form the Moon. The impactor presumably had already differentiated, and numerical simulations suggest that its core would have combined with the Earth's core, whereas parts of its mantle would have been blown away to eventually form the Moon.

The Moon's strong depletion in volatile elements provides geochemical evidence for the large impact hypothesis. For example, the lunar K–U and Rb–Sr ratios are a factor of approximately four lower than in the Earth. Not all of the orbiting vapor would have condensed, accounting for the scarcity of water, potassium, rubidium, and other volatile components. The oxygen isotopic composition of lunar samples deviates only very slightly from the Earth's mass fractionation line, suggesting that the impactor and the Earth originated in the same nebular neighborhood, or were efficiently mixed during the collision.

### 5.6.2 Orbital Scrambling

The Moon-forming impact was gigantic, but impacts of other massive bodies to create large basins occurred later on the Moon itself, as well as on Mercury, Venus, and Mars (and on Earth, although the record has been erased by geologic processes). Dating of these large impacts is based mostly on lunar rocks returned by *Apollo* astronauts. This has led to the concept of a **Late Heavy Bombardment** that appears to have ended at about 3.9 Ga. However, there has been considerable disagreement about whether the bombardment was a Solar System-wide punctuated event or represents a gradually declining, protracted accretion of ever-larger objects. In any case, the radial mixing of asteroid spectral classes (Figure 5.16) and the scattering of cometary bodies originally formed within the giant planet region into the Kuiper belt also point to a dynamic, rather than static, Solar System.

The need for a way to perturb large asteroids into the inner Solar System and eject comets outward into the Kuiper belt has prompted models that explore the possible orbital migration of the giant planets. Two possible models are illustrated in Figure 5.22. The Grand Tack model (Walsh et al., 2011) posits the inward and then outward migration of Jupiter and Saturn during the nebula phase; the name alludes to a sailing maneuver for changing direction. Gravitational interactions with inward-drifting Jupiter would have scrambled the orbits of smaller objects in the accretion disk, and ejected many of them from the Main belt. This model accounts for the otherwise puzzling small size of Mars and the asteroid belt, by depleting these regions of planetary

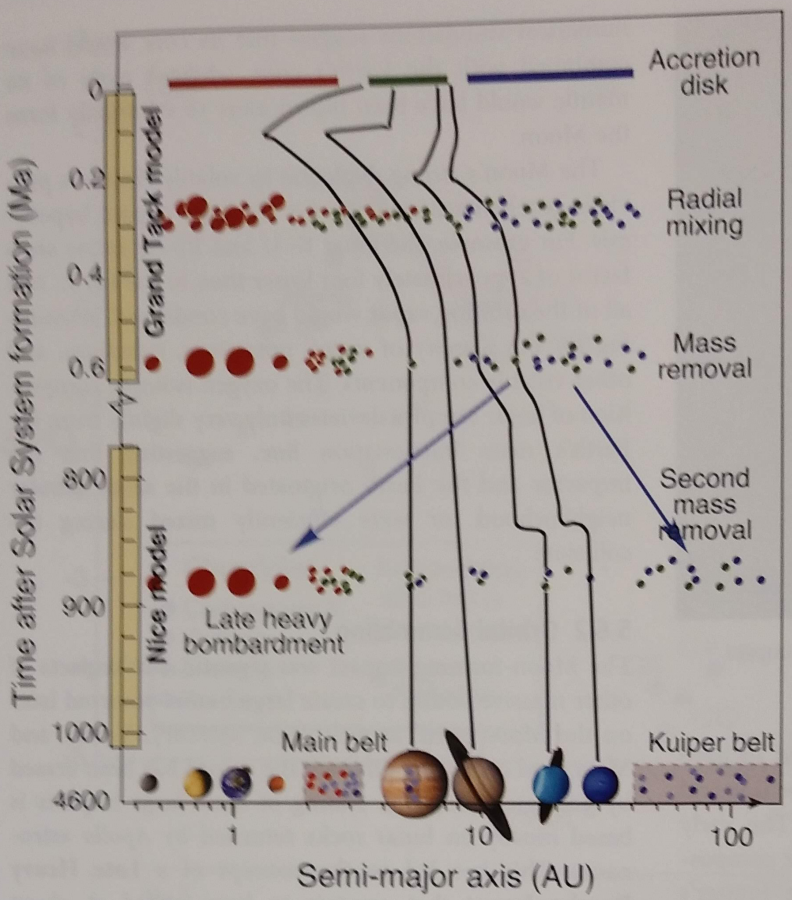


**Figure 5.22** The effects of orbital migrations of the giant planets, called the Grand Tack and Nice models, on planetesimals in the early accretion disk and later on asteroids in the Main belt. Modified from DeMeo and Carry (2014).

building materials. The Nice model (based on a trio of papers published in 2005) describes later wanderings of the giant planets, reshuffling asteroid orbits and sending them careening into the inner Solar System, where they could impact the terrestrial planets (perhaps accounting for the Late Heavy Bombardment). Icy bodies formed in the more collision-rich giant planet region could also have been scattered outward to the Kuiper belt by migrations of Uranus and Neptune. Planetary dynamic models are providing a new paradigm for Solar System evolution that has implications for how planetary geology is interpreted.

## Summary

The planetary system formed from coagulation of gas and dust into planetesimals and then planets within an accretion disk. The timescale for the Solar System has been determined from measuring radiogenic isotopes in meteorites; its age, based on the earliest solids (CAIs), is ~4.567 billion years, and planet formation was complete in a few tens of millions of years. The terrestrial planets are broadly chondritic in composition, but are depleted in volatile elements. This characteristic may have been inherited if they accreted from already differentiated protoplanets. The giant planets have much greater proportions of volatiles; Jupiter and Saturn accreted hydrogen and helium directly from the nebula, and Uranus and Neptune accumulated large quantities of ices. Asteroids and comets represent leftover planetary building blocks. A very large impact into the Earth is thought to have formed the Moon. Asteroid impacts onto other planets, as well as scattering of icy bodies into the outer Solar System, may have resulted from orbital scrambling by migrations of the giant planets.

## Review Questions

1. What is an accretion disk, and how does it evolve into a planetary system?
2. What do observations of young stars and numerical simulations of accretion reveal about planet formation?
3. Why do we use refractory inclusions to date the age of the Solar System, and what is its age?
4. How are short-lived and long-lived radionuclides used in combination to determine the timing of early solar system processes?
5. What evidence suggests that the Solar System has experienced a dynamic orbital evolution?

## SUGGESTIONS FOR FURTHER READING


Burbine, T. H. (2017) *Asteroids*. Cambridge: Cambridge University Press. A modern summary of asteroid astronomy, composition, physical properties, and impact threat.

DeMeo, F. E., and Carry, B. (2014) Solar System evolution from compositional mapping of the asteroid belt. *Nature*, **505**, 629–634. A very accessible review of models predicting the scrambling of asteroid orbits and the Late Heavy Bombardment.

Halliday, A. N. (2004) The origin and earliest history of the Earth. In *Treatise on Geochemistry*, Vol. 1, *Meteorites, Comets, and Planets*, ed. Davis, A. M. Oxford: Elsevier, pp. 509–557. An excellent summary of constraints on the age of our planet.

Libourel, G., and Corrigan, C. M. (2014) Asteroids: new challenges, new targets. *Elements*, **10**, 11–17. This paper and the following papers in the same issue are short and easy-to-digest introductions to properties, spectra, and composition of asteroids.

Morbidelli, A., Lunine, J. I., O'Brien, D. P., et al. (2012) Building terrestrial planets. *Annual Review of Earth and Planetary Sciences*, **40**, 251–275. A nice description of our current understanding of planetary accretion models.

Taylor, G. J. (2013) The bulk composition of Mars. *Chemie der Erde*, **73**, 401–420. A wonderful review of the methods by which planetary bulk compositions are determined.

Tolstikhin, I., and Kramers, J. (2008) *The Evolution of Matter*, Cambridge: Cambridge University Press. This book provides a rigorous explanation of planetary accretion and compositions.


## REFERENCES


Albarede, F. (2009) *Geochemistry*, 2nd edition. Cambridge: Cambridge University Press.

Amelin, Y., Krot, A. N., Hutcheon, I. D., et al. (2002) Lead isotopic ages of chondrules and calcium-aluminum-rich inclusions. *Science*, **297**, 1678–1683.

Barboni, M., Boehnke, P., Keller, B., et al. (2017) Early formation of the Moon 4.51 billion years ago. *Science Advances*, **3**, e1602365.

Borg, L. E., Gaffney, A. M., and Shearer, C. K. (2015) A review of lunar chronology revealing a preponderance of 4.34–4.37 Ga ages. *Meteoritics & Planetary Science*, **50**, 715–732.

Brownlee, D. (2014) The Stardust mission: analyzing samples from the edge of the Solar System. *Annual Review of Earth and Planetary Sciences*, **42**, 179–205.

Burbine, T. H. (2017) *Asteroids*. Cambridge: Cambridge University Press.

DeMeo, F. E., and Carry, B. (2014) Solar System evolution from compositional mapping of the asteroid belt. *Nature*, **505**, 629–634.

Halliday, A. N. (2004) The origin and earliest history of the Earth. In *Treatise on Geochemistry*, Vol. 1, *Meteorites, Comets, and Planets*, ed. Davis, A. M. Oxford: Elsevier, pp. 509–557.

Kruijer, T. S., Touboul, M., Fischer-Godde, M., et al. (2014) Protracted core formation and rapid accretion of protoplanets. *Science*, **344**, 1150–1154.

Kruijer, T. S., Kleine, T., Borg, L. E., et al. (2017) The early differentiation of Mars inferred from Hf–W chronometry. *Earth & Planetary Science Letters*, **474**, 345–354.

McSween, H. Y., and Huss, G. R. (2010) *Cosmochemistry*. Cambridge: Cambridge University Press.

Morbidelli, A., Lunine, J. I., O'Brien, D. P., et al. (2012) Building terrestrial planets. *Annual Review of Earth and Planetary Sciences*, **40**, 251–275.

O'Brien, D. P., Morbidelli, A., and Levinson, H. F. (2006) Terrestrial planet formation with strong dynamical friction. *Icarus*, **184**, 39–58.

Righter, K., Drake, M. J., and Scott, E. R. D. (2006) Compositional relationships between meteorites and terrestrial planets. In *Meteorites and the Early Solar System II*, eds. Lauretta, D. S., and McSween, H. Y. Tucson, AZ: University of Arizona Press, pp. 803–828.

Russell, C. T., McSween, H. Y., Jaumann, R., et al. (2015) The Dawn mission to Vesta and Ceres. In *Asteroids IV*, eds. Michel, P., DeMeo, F. E., and Bottke, W. F. Tucson, AZ: University of Arizona Press, pp. 419–432.

Russell, C. T., Raymond, C. A., Ammannito, E., et al. (2016) Dawn arrives at Ceres: exploration of a small, volatile-rich world. *Science*, **353**, 1008–1010.

Scott, E. R. D., Krot, A. N., and Sanders, I. S. (2018) Isotopic dichotomy among meteorites and its bearing on the protoplanetary disk. *The Astrophysical Journal*, **854**, 164–176.

Taylor, G. J. (2013) The bulk composition of Mars. *Chemie der Erde*, **73**, 401–420.

Tera, F. (1980) Reassessment of the "Age of the Earth". *Carnegie Institution of Washington Year Book*, **79**, 524–531.

Tolstikhin, I., and Kramers, J. (2008) *The Evolution of Matter*, Cambridge: Cambridge University Press.

Walsh, K. J., Morbidelli, A., Raymond, S. N., et al. (2011) Sculpting the inner Solar System by gas-driven orbital migration of Jupiter. *Nature*, **475**, 206–209.

Wang, H., Weiss, B. P., Bai, X-N., et al. (2017) Lifetime of the solar nebula constrained by meteorite paleomagnetism. *Science*, **355**, 623–627.

Warren, P. H. (2011) Stable-isotopic anomalies and the accretion assemblage of the Earth and Mars: A subordinate role for carbonaceous chondrites. *Earth and Planetary Science Letters*, **311**, 93–100.

Williams, D. A., Blewett, D. T., Buczkowski, D. L., et al. (2015) Complete global geologic map of Vesta from Dawn and mapping plans for Ceres. *Lunar and Planetary Science Conference*, **46**, 1126.

Williams, D. A., Buczkowski, D. L., Crown, D. A., et al (2018) High-resolution global geologic map of Ceres from NASA Dawn mission. In *Planetary Geologic Mappers Annual Meeting*. Houston, TX: Lunar and Planetary Science Institute, abstract 7001.